

文章编号:1001-9014(2021)01-0019-06

DOI:10.11972/j.issn.1001-9014.2021.01.004

卷曲量子阱红外探测器应力变化及对探测性能的影响

张 飞^{1,2,3}, 黄高山^{2*}, 聂晓飞⁴, 甄红楼⁴, 梅永丰², 范润华^{1,3*}

(1. 上海海事大学 海洋科学与工程学院, 上海 201306;

2. 复旦大学 材料科学系, 上海 200433;

3. 上海海事大学 上海深远海洋装备材料工程技术研究中心, 上海 201306;

4. 中国科学院上海技术物理研究所 红外物理国家重点实验室, 上海 200083)

摘要:研究了卷曲量子阱红外探测器的应力状态变化及对光电性能的影响,发现拉应力使导带能级上移,压应力则使其下移,且双量子阱结构的卷曲薄膜的能带移动取决于两个量子阱的合应力变化;卷管薄膜可以有效将应力变化转变为应变,从而减小环境温度变化对能带移动的影响,提高红外器件温度稳定性;褶皱薄膜相比卷管薄膜的量子阱具有较大的压应力,导致其光响应率较低;相同外加偏压下,卷管器件比褶皱器件的电压响应率提高约2.5倍。

关 键 词:量子阱红外探测器; 卷曲薄膜; 光致发光谱; 应力; 响应率

中图分类号:TN21 文献标识码: A

Stress evolution and its effects on the detection performance of self-rolled quantum well infrared detector

ZHANG Fei^{1,2,3}, HUANG Gao-Shan^{2*}, NIE Xiao-Fei⁴, ZHEN Hong-Lou⁴, MEI Yong-Feng², FAN Run-Hua^{1,3*}

(1. College of Ocean Science and Engineering, Shanghai Maritime University, Shanghai 201306, China;

2. Department of Materials Science, State Key Laboratory of ASIC and Systems, Fudan University, Shanghai 200433, China;

3. Shanghai Engineering Technology Research Centre of Deep Offshore Material, Shanghai Maritime University, Shanghai 201306, China;

4. State Key Laboratory of Infrared Physics, Shanghai Institute of Technical Physics, Chinese Academy of Sciences, Shanghai 200083, China)

Abstract: In this study, we investigate the stress evolution and its effects on the detection performance of self-rolled quantum well infrared detector. It is found that tensile stress can move the energy level of conduction band up, while compressive stress moves it down. The band movement of self-rolled film with double quantum wells depends on the change of resultant stresses in the two quantum wells. The rolled-up sample can effectively transform the stress change into strain, so as to weaken the impact of ambient temperature and enhance the stability of infrared devices. The wrinkled film has higher compressive stress compared with the rolled-up sample, which results in lower responsivity. When the same bias voltage is applied, the voltage responsivity of the rolled-up sample is about 2.5 times higher than that of the wrinkled sample.

Key words: quantum well infrared detector, rolled-up film, photoluminescence spectrum, stress, responsivity

PACS: 61.72.uj, 73.21.Fg, 78.30.Fs, 78.67.De

收稿日期:2020-07-13,修回日期:2020-11-25

Received date:2020-07-13, Revised date:2020-11-25

基金项目:国家自然科学基金(61805042, 61975035, U1632115);上海市基金(20ZR1423400, 18ZR1405100, 17JC1401700, 19XD1400600)

Foundation items: National Natural Science Foundation of China (61805042, 61975035, U1632115), Shanghai Project (20ZR1423400, 18ZR1405100, 17JC1401700, 19XD1400600)

作者简介(Biography):张飞(1986-),男,河南商丘人,上海海事大学讲师,主要从事光电材料物理及器件研究. E-mail: zhangfei@shmtu.edu.cn

*通讯作者(Corresponding author): E-mail: gshuang@fudan.edu.cn; rhfan@shmtu.edu.cn

引言

基于GaAs/AlGaAs量子阱结构的红外探测器具有抗辐射性能好,光谱响应带宽窄,波长连续可调等优异性能^[1-4]。但由于只有电矢量平行于量子阱生长方向入射光对光电流信号有贡献,因此,光能量利用率低,是限制器件的量子效率的重要因素^[5]。

卷曲纳米技术是2000年以来发明和兴起的一种新的纳米技术^[6]。该技术主要采用传统的剥离(lift-off)工艺的原理,利用薄膜本身的应力,将二维自由展开的纳米薄膜卷曲成微米或者纳米尺度的管子或者褶皱等结构^[7-10],目前已被用于气体探测^[11]、微电机^[12]、表面增强拉曼散射^[13]等方面。而将卷曲纳米技术与量子阱红外探测器结合,即将包含量子阱结构的柔性纳米薄膜卷曲形成管状或褶皱结构,不仅可以有效提高量子阱红外探测器的探测角^[14],并且可以增加光在微腔内的反射而提高其吸收率,进而提高量子阱红外探测器的量子效率^[15-16]。薄膜的卷曲必然会导致其应力状态发生变化,改变其能带结构,进而影响到薄膜材料或器件的物理性质^[17-20]。

将针对不同应力状态下的卷曲GaAs/AlGaAs量子阱红外器件的光电特性进行分析,发现能带移动随应力变化特点,并进行了相关机理的分析,进一步完善了卷曲量子阱红外器件在这一领域的理论,对制备高性能特点的卷曲量子阱器件具有一定指导意义。

1 实验

采用分子束外延生长法在GaAs(100)衬底上生长复合薄膜,其结构从下向上依次为牺牲层AlAs(30 nm)、应力层In_{0.2}Al_{0.2}Ga_{0.6}As(20 nm)、下电极层GaAs(50 nm)、量子阱功能层GaAs(6.5 nm)/Al_{0.26}Ga_{0.74}As(30 nm)、上电极层GaAs(20 nm),其中,功能层为双量子阱结构。电极结构为AuGe(50 nm)/Ni(25 nm)/Au(150 nm),其后退火温度为380~420 °C。本文中,采用浓度为13%~18%的HF酸溶液对AlAs牺牲层进行刻蚀,此时应力层In_{0.2}Al_{0.2}Ga_{0.6}As的应力得以释放,复合薄膜最终卷曲形成卷管(图1)或褶皱。

制备了褶皱薄膜以及直径分别为158、150、127、100、62 μm的卷管薄膜的量子阱红外器件。采用黑体响应测试系统测试试样对800 K黑体辐射源的红外响应。采用傅里叶变换红外光谱仪(Nicolet

6700)分别在40 K和70 K温度下测试试样的光电流谱,对卷管薄膜做显微红外检测和扫描电镜观测,测试区域约为50×150 μm²。采用LabRAM HR拉曼光谱仪(540 nm激光)测试褶皱薄膜和卷管薄膜的光致发光谱(Photoluminescence, PL谱)。

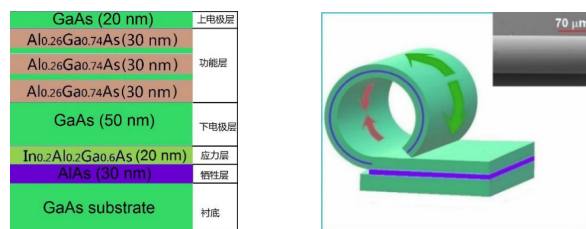


图1 复合薄膜层(左)及卷曲量子阱红外器件(右)示意图.右图中,蓝色的曲线为中位线,是压应力(红色箭头)和拉应力(绿色箭头)的过度区域,处于零应力状态.卷管外侧为拉应力,内侧为压应力。右上角插图为量子阱卷管薄膜的SEM图

Fig. 1 Schematic diagrams of multi-layer films (left) and rolled-up quantum well infrared device (right). The blue curve is the neutral line which is the boundary between tensile stress (green arrows) and compressive stress (red arrows) in the right diagram. The SEM image (top view) of rolled-up quantum well nanomembrane is in the top right inset

2 实验结论与分析

图2(a)为不同卷曲直径量子阱薄膜的PL谱,(b)~(f)为PL谱的分峰拟合,其中,e₀和e₁分别为导带的基态能级和激发态能级,hh₀和hh₁分别为价带的基态能级和激发态能级。各分峰分别对应卷管薄膜的带间跃迁峰e₀-hh₀,e₀-hh₁,e₁-hh₀,e₁-hh₁。对各卷管薄膜的PL谱分峰拟合的决定系数(coefficient of determination, COD)都为~0.999,说明所有的拟合数据可靠性较高。分析拟合所得卷管的带间跃迁峰值,可以得到各峰值随量子阱薄膜卷曲直径的变化(图3(a))和导带(Δe)和价带(Δhh)的带内跃迁能随薄膜卷曲直径的变化(图3(b))。由于薄膜存在两个量子阱,故卷管薄膜的某一带间跃迁峰其实是这两个量子阱各自带间跃迁峰所形成的合峰,故处于不同应力状态的两个量子阱的合应力效果(拉应力或压应力)决定了能级跃迁的红移或蓝移。比较图3(a)和图3(b),可以发现,随着卷曲半径的减小,图3(b)的带内跃迁能发生红移,根据文献[15]可知,拉应力使得带内跃迁产生红移,可知两个量子阱的合应力呈现为拉应力,而图3(a)的带

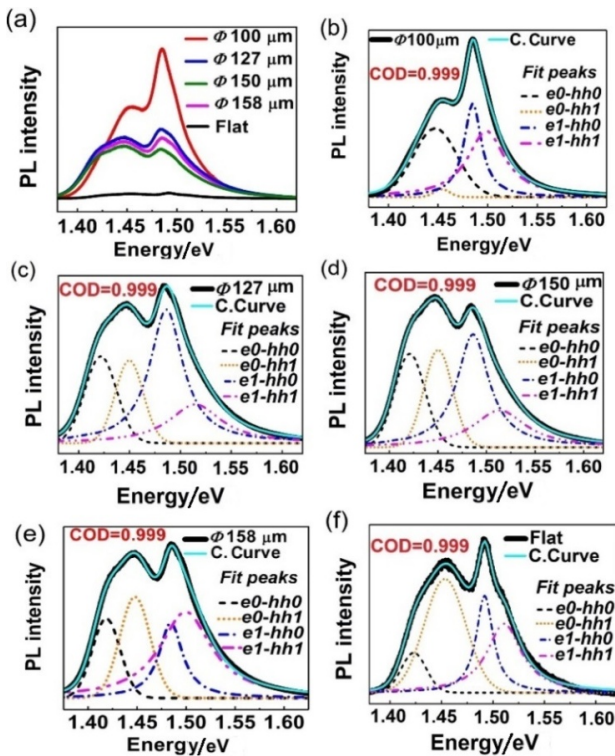


图2 (a)不同直径量子阱卷管薄膜的PL谱,(b)~(f)为PL谱的分峰拟合.总拟合曲线(Cumulative Curve)简写为C. Curve

Fig. 2 (a) PL spectra of rolled-up nanomembranes with different diameters, (b)~(f) are the fitting curves of PL spectra. “Cumulative Curve” is abbreviated as “C. Curve”

间跃迁则显示随卷曲半径减小跃迁能是蓝移。由此可得,拉应力不仅使得导带能级上移,而且基态上移幅度大于激发态能级;反之,压应力则应使得导带能级下降,且基态能级下降幅度会大于激发态能级(图3(c))。这主要由于应力改变了量子阱薄膜的原子间距,进而改变了限制势^[21~22],且电子能级的变化大于空穴能级^[23]。由于应力层的存在,未卷薄膜试样的两个量子阱最初都处于压应力状态^[15]。在薄膜卷曲过程中,内侧量子阱的压应力自始至终是一直增大的,而外侧量子阱则存在一个由压应力向拉应力的转变过程,使得最终卷曲成的管状试样内侧量子阱处于压应力状态,卷管外侧量子阱处于拉应力状态(图1)。由于卷管薄膜的各带间跃迁峰 $e_0-hh_0, e_0-hh_1, e_1-hh_0, e_1-hh_1$ 都是两个量子阱的合峰,故峰值变化取决于两个量子阱总体的应力状态,这就需要分析两个量子阱合应力状态变化。

图3(a)显示,未卷薄膜试样(Flat)开始卷曲后,带间跃迁先发生红移,说明薄膜卷曲开始时合应力是增大的压应力;其后随着卷曲直径的减小(158

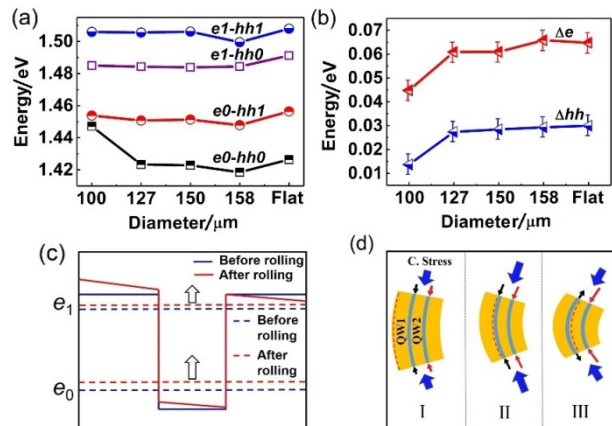


图3 (a)带间跃迁分峰的峰值随量子阱薄膜卷曲直径的变化,(b)导带(Δe)和价带(Δhh)带内跃迁随量子阱薄膜卷曲直径的变化,(c)拉应力状态下,量子阱导带边能带移动示意图,薄膜卷曲后 e_0 和 e_1 都上移,但 e_0 能级上移幅度大于 e_1 能级,(d)红色虚线为中位线位置,Part I:卷曲刚开始时,中位线位于最外侧,Part II:中位线移至QW₁外侧,Part III:中位线位于QW₁和QW₂之间. 黑色箭头表示QW₁受力,红色箭头表示QW₂受力,蓝色大箭头表示两量子阱对外显示的合应力(Comulative Stress简写为C. Stress)

Fig. 3 (a) Interband transition peak changes with the diameter of rolled-up nanomembrane; (b) Intraband transition peaks (conduction band Δe , Valence band Δhh) change with the diameter of rolled-up nanomembrane; (c) The movement of conduction band under tensile stress. After rolling, both of energy levels (e_0 and e_1) move up and e_0 moves more; (d) The red dotted line is the neutral line. Part I: The neutral line is at the outermost at the beginning of rolling. Part II: The neutral line moves to the outside of QW₁. Part III: The neutral line moves between QW₁ and QW₂. Black arrows indicate the stress in QW₁ and red arrows indicate the stress in QW₂. The blue arrows indicate the resultant stresses in the two quantum wells. “Comulative Stress” is abbreviated as “C. Stress”

μm 到100 μm)发生蓝移,说明在这一直径范围内($< 158 \mu\text{m}$)试样量子阱的合压应力随着卷曲直径的减小发生减小。这种应力变化对导带带内跃迁的影响在图3(b)中也较为明显的显现出来——先增大后减小的合压应力导致导带的带内跃迁能先蓝移后红移。这表明薄膜在开始卷曲时,外侧的量子阱最初是压应力,即中位线最初是位于外侧量子阱的外侧(图3(d)的I部分),此时量子阱的合应力为压应力;当薄膜应力释放后开始卷曲时(由图3(d)的I向II部分变化),两个量子阱的压应力都增大,合压应力也是增大的;随着卷曲直径的继续减小(由图3(d)的II向III部分变化),中位线开始跨过QW₁,此

时的QW₁压应力开始减小,导致在这一变化过程中两个量子阱合压应力逐渐减小。到小于158 μm时,中位线已经位于两个量子阱之间^[15],即外侧量子阱QW₁完全处于拉应力。

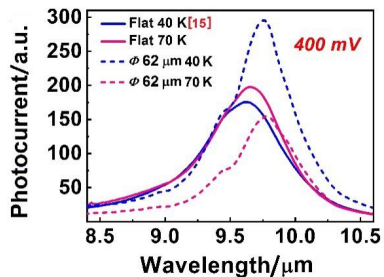


图4 未卷薄膜和62 μm卷曲直径的红外探测器在400 mV外加偏压下,分别在40 K和70 K工作温度下的光电流谱

Fig. 4 Photocurrent spectra of infrared detectors for flat and rolled-up (diameter: 62 μm) nanomembranes under 400 mV applied voltage, collected at 40 and 70 K separately

应力变化会引起能带移动,而卷管试样则可以有效将应力变化转变为应变,从而减小能级的漂移,提高器件的性能稳定性。如我们分别在40 K和70 K温度下测试未卷薄膜和62 μm直径卷曲量子阱红外器件,从图4可以看出,未卷薄膜器件的光电流谱在70 K时相比在40 K时红移0.000 48 eV,而62 μm的卷管器件则是红移0.000 24 eV,说明卷管器件光电性能更稳定,具有较好地抗温度波动性。主要是由于卷管薄膜处于悬空状态,在升温过程中可以有效将增大的应力转为应变,降低环境温度所引起的薄膜的应力浮动,减小环境温度变化对能带移动的影响,进而提高其器件稳定性,这对于性能稳定的非制冷型量子阱红外器件的研制具有重要意义。

我们对卷管薄膜和褶皱薄膜的性能进行对比分析。实验中制备的褶皱薄膜试样如图5(a)所示,为了对图中虚线对应的褶皱部分进行进一步分析,我们选取几个点(如图5(b)所示)进行PL谱分析。我们测得未卷薄膜的PL谱峰值为1.488 9 eV^[24],可以看出,所有的点相比于未卷时都是发生红移,所以褶皱薄膜两个量子阱的合应力相比于未卷薄膜是增大的压应力。从图5(b)可以看出,曲率半径较小的C点红移最大,说明其总压应力最大,而A和B点分别位于较大的曲率半径薄膜的顶部,其压应力相对较小,所以红移相对较小,这符合两个量子阱都处于压应力的应力变化规律,即中位线位于图3

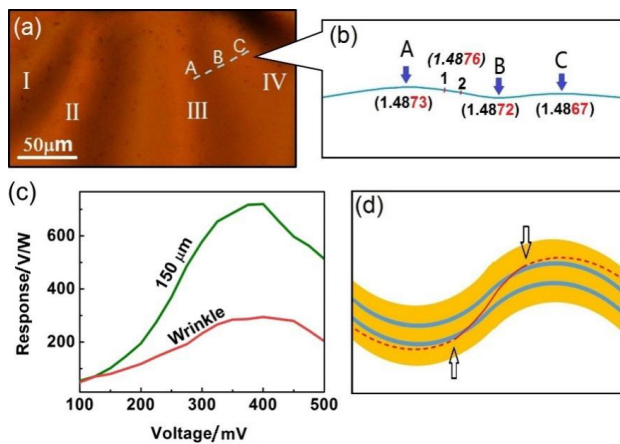


图5 (a) 褶皱薄膜的显微光学图片(俯视),其凸起部分已经被标注“I”,“II”,“III”,“IV”。右上角红线对应的剖视图如图(b)所示,其中A,C为褶皱的峰,B为谷,“1”,“2”为A,B两点的中间部分所取两点。图中括号内为这些点所对应的PL谱峰值,单位为eV。其中,1,2两点PL谱的峰值位置相同,(c) 150 μm卷管红外器件和褶皱器件的光响应率对比图,(d)红色的线为中位线。其中,虚线部分对应的两个量子阱都为压应力,而两个箭头中间的实线所对应的量子阱部分一个为压应力,另一个为拉应力,是应力过渡区

Fig. 5 (a) Optical microscopy image of wrinkled nanomembrane (top view). The peaks of raised parts are marked with “I”, “II”, “III” and “IV”. Figure (b) is the section view of the red dotted line in the top right corner of Figure (a). A, C points are the peaks and B point is the valley. “1”, “2” points are between A and B points. The values (unit: eV) in the brackets are the peaks of their PL spectra, where the peak positions are the same for “1” and “2” points, (c) Comparison of blackbody responsivity between rolled-up nanomembrane detector (diameter: 150 μm) and the wrinkled nanomembrane detector, (d) The red line is neutral line and the quantum wells in the dotted neutral line regions are both compressive. For the quantum wells in middle solid neutral line region, one quantum well is compressive, and the other is in tensile stress

(d)中part I所示的位置。因为如果两个量子阱分别为压应力和拉应力,则随着曲率半径的减小PL峰会发生蓝移。

由于此时褶皱的峰和谷位置薄膜的两个量子阱都是压应力,必然存在一个过渡区使得中位线位于两个量子阱中间,即一个拉应力、另一个压应力状态(图5(d)),其合应力相比于A、B点较小,即其PL谱红移更小。我们选取A、B两点中间的1、2两点(如图5(b)所示),可以看出两点位置的PL谱相比于A、B两点确实发生了更小的红移。褶皱薄膜的这种应力分布状态必然会影响褶皱薄膜器件的

光电性能。我们分别制备了卷曲和褶皱的量子阱薄膜器件以便于对比。实验结果显示,两者都在400 mV外加偏压下具有最高值,但卷管薄膜器件比褶皱薄膜器件的电压响应率高约2.5倍(图5(c))。我们由文献[15]得出,拉应力状态的量子阱具有较大的光电流响应,150 μm卷曲薄膜的量子阱一个处于拉应力,另一个处于压应力;而实验所得褶皱薄膜曲率相比较小,导致其峰和谷的薄膜部分两个量子阱都处于压应力状态(即由图3(d)的I向II部分变化),只有两者之间的过渡区域是一个压应力,另一个拉应力(图5(d)),故褶皱薄膜的量子阱具有相对较大的压应力,导致其光响应率较低。

3 结论

通过对卷曲薄膜的应力状态及光电性能分析,发现拉应力使得薄膜的导带能级上移,且基态上移幅度大于激发态能级;而压应力则使得导带能级下降,且基态能级下降幅度大于激发态能级;双量子阱结构的卷曲薄膜的能带移动则取决于两个量子阱的合应力变化。通过对未卷薄膜和卷管薄膜的红外探测器在不同温度下的光电流谱进行测试,发现卷曲器件可以有效将应力变化转变为应变,从而减小环境温度变化对能带移动的影响,提高红外器件稳定性,这对于性能稳定的非制冷型量子阱红外器件的研制具有重要意义。还对褶皱薄膜也进行了应力分析,发现褶皱薄膜相比于卷曲薄膜具有相对较大的压应力,导致其红外探测器件光响应率较低。在相同外加偏压下,卷管器件比褶皱器件的电压响应率提高约2.5倍。

References

- [1] Lin L, Zhen H L, Zhou X H, et al. An intermediate-band-assisted avalanche multiplication in InAs/InGaAs quantum dots-in-well infrared photodetector [J]. *Applied Physics Letters*, 2011, **98**(7): 073504.
- [2] Makhov I S, Panarin V Y, Sofronov A N, et al. The effect of stimulated interband emission on the impurity-assisted far-infrared photoluminescence in GaAs/AlGaAs quantum wells [J]. *Superlattice and Microstructures*, 2017, **112**: 79–85.
- [3] Cevher Z, Folkes P A, Hier H S, et al. Optimization of the defects and the nonradiative lifetime of GaAs/AlGaAs double heterostructures [J]. *Journal of Applied Physics*, 2018, **123**(16): 161512.
- [4] Li Q, Li Z F, Li N, et al. High-polarization-discriminating infrared detection using a single quantum well sandwiched in plasmonic micro-cavity [J]. *Scientific Reports*, 2014, **4**: 6332.
- [5] Fu Y, Willander M, Lu W, et al. Optical coupling in quantum well infrared photodetector by diffraction grating [J]. *Journal of Applied Physics*, 1998, **84**(10): 5750–5755.
- [6] Smith E J, Liu Z, Mei Y, et al. Oliver G. Schmidt. Combined Surface Plasmon and Classical Waveguiding through Metamaterial Fiber Design [J]. *Nano Letters*, 2010, **10**(1): 1–5.
- [7] Zhang J, Li J X, Tang S W, et al. Whispering-gallery nanocavity plasmon-enhanced Raman spectroscopy [J]. *Scientific Reports*, 2015, **5**: 15012.
- [8] Ning H P, Zhang Y, Zhu H, et al. Geometry design, principles and assembly of micromotors [J]. *Micromachines-based*, 2018, **9**(2): 75.
- [9] Huang W, Yu X, Froeter P, et al. On-chip inductors with self-rolled-up SiN_x nanomembrane tubes: a novel design platform for extreme miniaturization [J]. *Nano Letters*, 2012, **12**(12): 6283–6288.
- [10] Schmidt O G, Eberl K. Thin solid films roll up into nanotubes [J]. *Nature*, 2001, **410**: 168.
- [11] Xu B R, Tian Z A, Wang J, et al. Stimuli-responsive and on-chip nanomembrane micro-rolls for enhanced macroscopic visual hydrogen detection [J]. *Science Advances*, 2018, **4**: eaap8203.
- [12] Mei Y F, Huang G S, Alexander A S, et al. Versatile approach for integrative and functionalized tubes by strain engineering of nanomembranes on polymers [J]. *Advanced Materials*, 2008, **20**: 4085–4090.
- [13] Fan X C, Hao Q, Li M Z, et al. Hotspots on the Move: Active Molecular Enrichment by Hierarchically Structured Micromotors for Ultrasensitive SERS Sensing [J]. *ACS Appl. Mater. Interfaces*, 2020, **12**(25), 28783–28791.
- [14] Wang H, Zhen H L, Li S L, et al. Self-rolling and light-trapping in flexible quantum well-embedded nanomembranes for wide-angle infrared photodetectors [J]. *Scientific Reports*, 2016, **2**: e1600027.
- [15] Zhang F, Nie X F, Huang G S, et al. Strain-modulated photoelectric properties of self-rolled GaAs/Al_{0.26}Ga_{0.74}As quantum well nanomembrane [J]. *Applied Physics Express*, 2019, **12**(6): 065003.
- [16] Dietrich K, Strelow C, Schliehe C, et al. Optical Modes Excited by Evanescent-Wave-Coupled PbS Nanocrystals in Semiconductor Microtube Bottle Resonators [J]. *Nano Letters*, 2010, **10**(2): 627–631.
- [17] Wong J H, Wu B R, Lin M F. Strain effect on the electronic properties of single layer and bilayer graphene [J]. *The Journal of Physical Chemistry C*, 2012, **116**(14): 8271–8277.
- [18] Deneke C, Malachias A, Kiravittaya S, et al. Strain states in a quantum well embedded into a rolled-up microtube: X-ray and photoluminescence studies [J]. *Applied Physics Letters*, 2010, **96**(14): 143101.
- [19] Strelow C, Schultz C M, Rehberg H, et al. Light confinement and mode splitting in rolled-up semiconductor microtube bottle resonators [J]. *Physical Review B*, 2012, **85**(15): 155329.
- [20] Xu B R, Zhang X Y, Tian Z A, et al. Microdroplet-guided intercalation and deterministic delamination towards intelligent rolling origami [J]. *Nature Communications*, 2019, **10**: 5019.
- [21] Ganawan O, Djie H S, Ooi B S. Electronic states of inter-

- diffused quantum dots [J]. *Physical Review B*, 2005, **71**(20): 205319.
- [22] Xu S J, Wang H, Li Q, et al. X-ray diffraction and optical characterization of interdiffusion in self-assembled InAs/GaAs quantum-dot superlattices [J]. *Applied Physics Letters*, 2000, **77**(14): 2130–2132.
- [23] Aziz-Aghcheghala V L, Pishbaz M, Effect of Interdiffusion on Optoelectronic Properties of $\text{In}_{1-x}\text{Ga}_x\text{As}/\text{InAs}/\text{In}_{1-y}\text{Al}_y\text{As}$ Quantum Well [J]. *Procedia Materials Science*, **2015**, **11**: 727–732.
- [24] Zhang F, Huang G S, Nie X F, et al. Energy Band Modulation of GaAs/ $\text{Al}_{0.26}\text{Ga}_{0.74}\text{As}$ Quantum Well in 3D Self-Assembled Nanomembranes [J]. *Physics Letters A*, 2019, **383**, 2938.